Spontaneous Emission and Fundamental Limitations on the Signal-to-Noise Ratio in Deep-Subwavelength Plasmonic Waveguide Structures with Gain

Andrey A. Vyshnevyy and Dmitry Yu. Fedyanin*

Laboratory of Nanooptics and Plasmonics, Moscow Institute of Physics and Technology, 141700 Dolgoprudny, Russian Federation

(Received 13 September 2016; published 29 December 2016)

Incorporation of gain media in plasmonic nanostructures can give the possibility to compensate for high Ohmic losses in the metal and design truly nanoscale optical components for diverse applications ranging from biosensing to on-chip data communication. However, the process of stimulated emission in the gain medium is inevitably accompanied by spontaneous emission. This spontaneous emission greatly impacts the performance characteristics of deep-subwavelength active plasmonic devices and casts doubt on their practical use. Here we develop a theoretical framework to evaluate the influence of spontaneous emission, which can be applied to waveguide structures of any shape and level of mode confinement. In contrast to the previously developed theories, we take into account that the spectrum of spontaneous emission can be very broad and nonuniform, which is typical for deep-subwavelength structures, where a high optical gain (approximately 1000 cm^{-1}) in the active medium is required to compensate for strong absorption in the metal. We also present a detailed study of the spontaneous emission noise in metal-semiconductor active plasmonic nanowaveguides and demonstrate that by using both optical and electrical filtering techniques, it is possible to decrease the noise to a level sufficient for practical applications at telecom and midinfrared wavelengths.

DOI: 10.1103/PhysRevApplied.6.064024

I. INTRODUCTION

Plasmonics have attracted great interest in the recent decade thanks to the unique opportunity to confine light to a space much smaller than the light wavelength by converting it into surface-plasmon polaritons (SPPs). This possibility of bringing optical signals to the nanoscale is highly important for the design of tiny photonic devices with dimensions approaching those of on-chip electronic components. However, the fundamental problem in plasmonics is absorption in the metal, which limits the propagation length of SPPs in passive deep-subwavelength plasmonic waveguide structures to a few tens of micrometers in the infrared and visible spectral ranges [1]. For practical application of plasmonic devices, the propagation length must be increased, which can be realized by surface-plasmon amplification by stimulated emission of radiation using a gain medium incorporated in the plasmonic structure [2]. The gain medium can be pumped either optically [2,3] or electrically [4,5], which creates population inversion, and, therefore, provides optical gain for SPPs. However, the process of stimulated emission is unavoidably accompanied by spontaneous emission [6]. Previously, spontaneous emission has been studied in a planar (1D) plasmonic waveguide geometry with weak mode confinement and with a gain medium in the form of dye molecules or rare-earth ions [7,8]. However, these results cannot be applied or generalized to nonplanar (2D) waveguides, where the SPP electromagnetic field is confined in both vertical and horizontal directions or to other types of gain media such as semiconductors. In addition, the material gain in the active medium required for loss compensation in deep-subwavelength plasmonic waveguides is 2 orders of magnitude greater than in the previously studied geometries [7,8]. These high values of optical gain in the active medium required for loss compensation in deep-subwavelength plasmonic waveguide structures result in high spontaneous emission rates. The stronger the SPP mode confinement, the higher the optical gain in the active medium required to compensate for losses in the metal and, consequently, the greater the power of spontaneous emission going into the SPP mode. Moreover, due to the randomness of the phase of the spontaneously emitted radiation, spontaneous emission can greatly increase the noise level, which may limit the applicability of active plasmonic waveguide structures [9]. Therefore, the study of spontaneous emission and noise in deep-subwavelength active plasmonic waveguide structures, where losses in the metal are compensated by optical gain in the active medium, is crucially important in designing and developing truly nanoscale photonic devices and components.

In this work, we develop a theoretical framework to study spontaneous emission and spontaneous emission noise in plasmonic waveguides with gain and in SPP amplifiers. We derive general expressions for the spontaneous emission at the output of the waveguide or amplifier, which can be utilized for any waveguide geometry. Using

*dmitry.fedyanin@phystech.edu

the quantum-optics formalism, we rigorously evaluate the spontaneous emission noise taking into account that the spontaneous emission spectrum can be very broad and have a complicated shape. Using the developed framework and numerical simulations, we examine the influence of the spontaneous emission noise on the characteristics and performance of truly nanoscale active plasmonic waveguides, where the SPP propagation losses are fully compensated by optical gain in the active medium, in a wide range of waveguide lengths and operation wavelengths, and analyze the possibility of practical application of active plasmonic structures. We find that due to the high optical gain in the active medium and, consequently, the high spontaneous emission rate, the spontaneous-spontaneous beat noise can drastically limit the applicability of nanoscale active plasmonic structures. At the same time, we demonstrate that optical filtering can suppress the spontaneous-spontaneous beat noise, while the signal-spontaneous beat noise can be controlled at a sufficiently low level.

II. SPONTANEOUS EMISSION INTO THE WAVEGUIDE MODE

Here, we mainly focus on deep-subwavelength plasmonic waveguides, which can provide the mode size below $\lambda^2/100$ and are promising for diverse on-chip applications. However, the derived theoretical equations can be applied with no change to any active plasmonic or nanophotonic waveguides. Because of the strong mode confinement in plasmonic waveguides, a significant part of the SPP electromagnetic field is concentrated in the metal. This results in high Ohmic losses, and the optical signal propagating along such a passive waveguide rapidly decreases with the distance from the transmitter (see Fig. 1). To avoid this strong attenuation, active media, which can support high material gain, should be used to compensate for the SPP propagation losses. Direct band-gap semiconductors, such as (InGa)As, are the best candidates for the role of the active medium in such deep-subwavelength structures [10]. In addition to the ability to provide a high material gain [11], they offer a large refractive index (approximately 3.5), which facilitates the improvement of the SPP mode confinement. Being pumped either optically or electrically, the semiconductor can possibly compensate fully for the SPP propagation losses [Fig. 1(b)]. However, in practice, one deals with optical signals of finite power. Moreover, it is usually highly desirable to reduce the signal power in order to enhance the energy efficiency of the devices. In this case, the contribution of spontaneous emission, which accompanies any stimulated emission, to the output power cannot be ignored [Fig. 1(b)], and, what is even more important, spontaneous emission can greatly increase the noise level.

To address this problem, we start our analysis with the spontaneous emission rate per unit waveguide length that

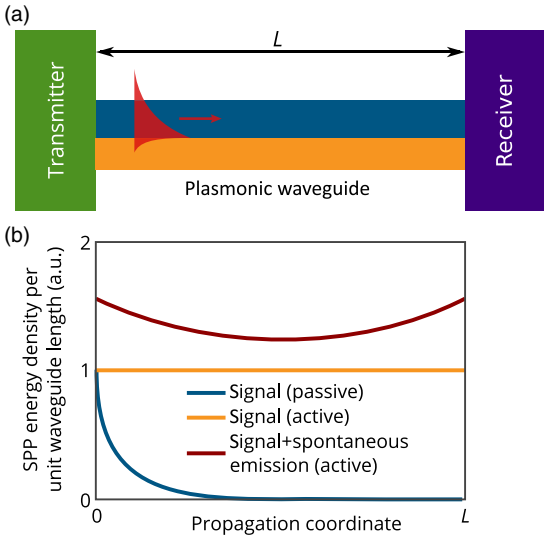

FIG. 1. (a) Schematic illustration of the plasmonic waveguide with gain, which connects the transmitter and receiver. (b) Qualitative dependence of the energy density of the SPP mode on the propagation coordinate in a passive waveguide (blue curve) in a sophisticated active plasmonic waveguide with full loss compensation (yellow curve) and in a real active plasmonic waveguide with full loss compensation (red curve). In the latter case, spontaneous emission can significantly contribute to the power of the SPP mode.

goes into the SPP mode. The spectral density of the spontaneous emission rate into the waveguide mode per unit waveguide length can be found using the Fermi golden rule:

$$R_{\mathrm{sp}}(h\nu) = \frac{\pi^2 e^2}{h m^2 c^2} \int_{\mathrm{active}} \left[\int_0^\infty f_2(E_2)[1 - f_1(E_1)] \times |M(E_1, E_2)|^2 \rho_v(E_1) \rho_c(E_2) dE_2 \right] \times |A_{\mathrm{WG}}(h\nu, x, y)|^2 \rho_{\mathrm{WG}}(h\nu) dx dy. \quad (1)$$

Here, the integration is performed over the active semiconductor region, e is the electron charge, m is the free-electron mass, c is the speed of light, E_1 and $E_2 = E_1 + h\nu$ are the energies in the valence and conduction bands of the semiconductor, respectively, f_1 and f_2 are the Fermi-Dirac distribution functions, which show the occupation probability of the states at energies E_1 and E_2. ρ_c and ρ_v are the density of states functions in the conduction and valence bands of the semiconductor, respectively, and $M(E_1, E_2)$ is the optical matrix element, which contains the electron wave functions of the initial and final states of the optical transition. Expression (1) is very similar to the expression for spontaneous emission in a bulk semiconductor medium [12] except that $A_{\mathrm{WG}}(h\nu, x, y)$ is the vector potential

normalized to one SPP quantum in the waveguide mode, and $\rho_{WG}(h\nu) = 2/(hv_g)$ is responsible for the density of optical states (DOS) in the waveguide (v_g is the group velocity of the SPP mode). This difference in the expression for spontaneous emission is attributed to the Purcell effect and can be described using the Purcell factor given by

$$F_P = \frac{|A_{WG}(h\nu, x, y)|^2 \rho_{WG}(h\nu)}{|A_0(h\nu)|^2 \rho_0(h\nu)}, \tag{2}$$

where $A_0(h\nu)$ is the vector potential normalized to one photon in a bulk medium, and $\rho_0(h\nu)$ is the DOS in a bulk semiconductor medium [the expressions for $A_0(h\nu)$ and $\rho_0(h\nu)$ can be found in Ref. [12]]. However, we avoid the Purcell factor formalism. Later, this gives us a possibility to directly connect the spontaneous emission rate into the SPP mode with the SPP modal gain.

The material gain can be easily found from the transition probabilities between electron states E_2 and E_1 in the conduction and valence bands of the semiconductor [12]:

$$g(h\nu) = \frac{2\pi e^2}{m^2 c n \nu} \int_0^\infty |M(E_1, E_2)|^2 [f_2(E_2) - f_1(E_1)] \times \rho_c(E_2)\rho_v(E_1) dE_2. \tag{3}$$

Combining Eqs. (1) and (3), we can express $R_{sp}(h\nu)$ in terms of the material gain in the active semiconductor medium:

$$R_{sp}(h\nu) = \frac{2}{h} \int_{active} \Gamma(h\nu, x, y) g(h\nu) \frac{1}{1 - \exp\left(\frac{h\nu - (F_e - F_h)}{k_B T}\right)} dxdy. \tag{4}$$

Here F_e and F_h are the quasi-Fermi-levels for electrons and holes, respectively, and $\Gamma_c = \int_{active} \Gamma(h\nu, x, y) dxdy$ is the SPP mode confinement to the active semiconductor region [13] so that the SPP modal gain can be found as [14]

$$G(h\nu) = \int_{active} g(h\nu)\Gamma(h\nu, x, y) dxdy.$$

Generally speaking, $g(h\nu)$ has a spatial distribution $g(h\nu, x, y)$ across the active region [7,15], but usually, it is quite uniform [12], and $g(h\nu, x, y) \cong g(h\nu)$. Taking this into account and integrating $R_{sp}(h\nu)$ over the waveguide length, we find the spectral density of spontaneous emission at the receiver [see Fig. 1(a)]:

$$p_{sp}(h\nu) = \nu \left(\frac{\exp\{[G(h\nu) - \alpha(h\nu)]L\} - 1}{G(h\nu) - \alpha(h\nu)} \right) \times \frac{G(h\nu)}{1 - \exp\left(\frac{h\nu - (F_e - F_h)}{k_B T}\right)}, \tag{5}$$

where $\alpha(h\nu)$ is the SPP modal loss associated with absorption in the metal and other energy-dissipation mechanisms. The expression in braces arises due to amplification of spontaneous emission, since the SPP quanta emitted spontaneously at a distance z from the receiver propagate over this distance in the active plasmonic waveguide with gain and can be amplified. Here we should emphasize that Eqs. (4) and (5) are valid for active media based on semiconductors, quantum wells, and low-dimensional semiconductors. They can be applied with no change to active nanophotonic waveguides of any shape, such as dielectric-loaded [16], hybrid [17], slot [18], T-shaped [19], and other plasmonic waveguides. Equations (4) and (5) can be easily adopted for active media based on atomiclike quantum systems (dye molecules, rare-earth ions, quantum dots). One needs only to replace the last term under the integral in Eq. (4) by the population inversion parameter:

$$\frac{1}{1 - \exp\left(\frac{h\nu - (F_e - F_h)}{k_B T}\right)} \to \frac{1}{1 - \frac{\sigma_a(h\nu) N_1}{\sigma_e(h\nu) N_2}}. \tag{6}$$

Here, $\sigma_e(h\nu)$ and $\sigma_a(h\nu)$ are the emission and absorption cross sections of individual emitters, respectively, N_1 is the population of the ground state, and N_2 is the population of the excited state [20].

The spontaneous emission power at the receiver is obtained by integrating $p_{sp}(h\nu)$ over all SPP frequencies:

$$P_{sp} = \int_0^\infty p_{sp}(h\nu) d(h\nu). \tag{7}$$

In order to minimize P_{sp}, it is reasonable to set the wavelength $\lambda_0 = c/\nu_0$ of the signal from the transmitter equal to the wavelength of the peak in the net SPP modal gain spectrum $G_{net}(h\nu) = G(h\nu) - \alpha(h\nu)$ and make the level of population inversion as low as possible, such that $G_{net}(h\nu) \le G_{net}(h\nu_0) = 0$. This regime can be referred to as the regime of full loss compensation. However, even in this case, the spontaneous emission power can be very high due to the high material gain in the semiconductor active region, which is required to compensate for the high Ohmic losses in deep-subwavelength plasmonic waveguides.

Below we present numerical results for the dielectric-loaded plasmonic waveguide with gain [Fig. 2(a)]. At the same time, we should note that approximately the same numbers are obtained for other true subwavelength waveguide geometries such as slot [21], hybrid [17], or T-shaped

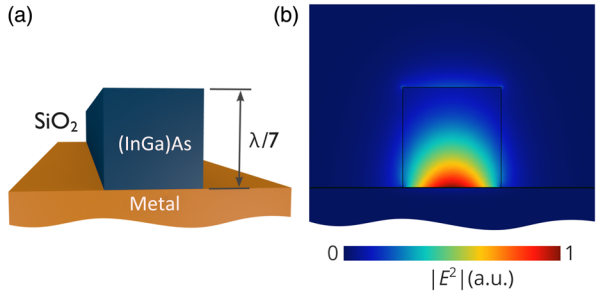

FIG. 2. (a) Schematic of the single-mode active dielectric loaded SPP waveguide based on copper as a metal and (InGa)As as an active semiconductor medium, where the population inversion can be created. Dimensions of the waveguide cross section are 7 times smaller than the signal wavelength (220×220 nm^2 for $\lambda_0 = 1550$ nm). (b) Electric-field-intensity ($|E|^2$) distribution of the SPP mode simulated at $\lambda_0 = 1550$ nm using the finite-element method.

[15] plasmonic waveguides. This is determined by the fundamental relationship between the SPP modal gain $G(h\nu)$ and the spontaneous emission rate into the SPP mode (which is also known as the Einstein relationship) and is confirmed by our calculations. The core of the studied waveguide has a square cross section with a side length of $\lambda_0/7$, where λ_0 is the free-space wavelength of the signal sent by the transmitter [see Fig. 1(a)]. The waveguide is designed to support only the fundamental SPP mode. The size of the waveguide for telecom applications is as low as 220×220 nm^2. The active gain medium is the ternary $In_xGa_{1-x}As$ alloy, which is very promising for near- to midinfrared applications [22–24]. The SPP supporting interface is formed using copper, which, according to the recent experimental studies, can outperform gold in the infrared [25,26] and is more attractive for practical applications. At the same time, we note that nearly the same results are obtained for gold waveguides. The mode size A of the SPP mode, defined as the ratio of the total mode energy to the peak energy density [17], in such a waveguide does not exceed $0.008\lambda_0^2$ at telecom wavelengths [see Fig. 2(b)], and the confinement is almost equally strong in the midinfrared: $A = 0.01\lambda_0^2$ at $\lambda_0 = 3$ μm. The chosen waveguide dimensions give the possibility of not only reducing the mode size but also achieving a high confinement of the SPP mode to the active semiconductor region: Γ_c ranges from 1.33 at 1550 nm to 1.19 at 3 μm. This facilitates a reduction in the material gain required to achieve full loss compensation ($G = 1300$ cm^{-1} and $g = 980$ cm^{-1} at $\lambda_0 = 1550$ nm) and, consequently, helps to decrease the spontaneous emission power. At the same time, in spite of the small mode size, the Purcell factor F_p [see Eq. (2)] averaged over the active semiconductor region is as low as approximately 0.35, which can be clearly seen in Fig. 3(a). Figure 3(a) also demonstrates that the spontaneous emission power at the

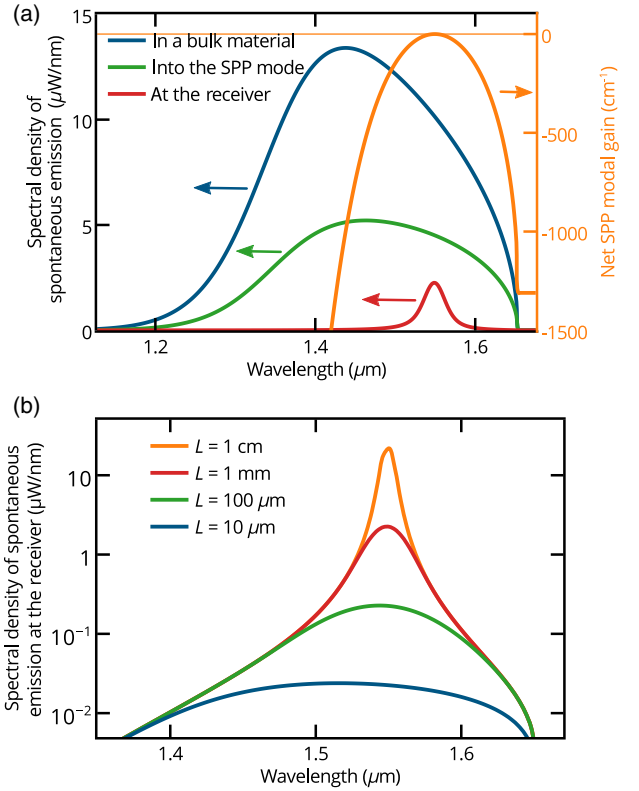

FIG. 3. (a) Spectrum of the net SPP modal gain $G_{net}(h\nu) = G(h\nu) - \alpha(h\nu)$ in the deep-subwavelength active plasmonic waveguide [Fig. 2(a)] in the regime of full loss compensation [$G_{net}(h\nu_0) = 0$] and curves for the spectral density of spontaneous emission. The length of the active plasmonic waveguide is as high as 1 mm, which is the typical size for chip-scale optical communication systems [27]. The green curve corresponds to the spontaneous emission that goes into the SPP mode, and the red curve corresponds to the spontaneous emission registered at the receiver. The blue curve shows the emission of the active semiconductor core in a homogeneous semiconductor medium. (b) Spectral density of spontaneous emission at the receiver for different lengths of the active plasmonic waveguide.

receiver is significantly lower than the spontaneous emission power going into the SPP mode, since the spontaneous emission spectrum in (InGa)As is much broader than the gain spectrum, and SPP quanta with wavelengths beyond the narrow band around λ_0 are strongly absorbed in both the metal and semiconductor. This is especially pronounced at long waveguide lengths [Fig. 3(b)]. The spontaneous emission spectrum at the receiver is 2.9 times narrower at $L = 1$ mm than at $L = 100$ μm, where L is the length of the active plasmonic waveguide [see Fig. 1(a)]. At $L = 1$ cm, the spectrum width is again 3.1 times smaller than at $L = 1$ mm. In spite of the reduction in the spectrum width, the total spontaneous emission power at the receiver steadily increases as the waveguide length increases: $P_{sp} = 25$ μW at $L = 100$ μm, $P_{sp} = 97$ μW at $L = 1$ mm, and $P_{sp} = 330$ μW at $L = 1$ cm. Our analysis also shows that P_{sp} is directly proportional to the square root of the

waveguide length at $L \gtrsim 200\ \mu$m, which can be explained as follows. The height of the peak in the spontaneous emission spectrum at the receiver, namely, the spectral density of spontaneous emission at $\lambda = \lambda_0$, is directly proportional to the waveguide length [see Fig. 3(b)], while the peak width is inversely proportional to the square root of the waveguide length due to the quadratic dependence of the material gain in the semiconductor in the vicinity of its maximum.

III. SPONTANEOUS EMISSION NOISE

High spontaneous emission power results in noise at the receiver, which is due to the fact that the photodetector of the receiver mixes the signal SPPs and the spontaneously emitted SPPs propagating in the waveguide coherently [28], despite that they are not coherent and do not interfere with each other. The photodetector converts the optical signal to the electrical current, and the spontaneous emission noise should be understood as the electrical current noise [28,29]. The common approach to estimate the noise produced by spontaneous emission is to consider dipolar emitters in the active medium as two-level systems, which produce spontaneous emission uniformly distributed over a narrow frequency band [30]. This technique can be used for active media doped with rare-earth ions or dye molecules, but it cannot be applied to semiconductors (bulk semiconductors, quantum wells, and low-dimensional semiconductors) and many other materials where spontaneous emission has a broad spectrum.

In order to evaluate the noise produced by spontaneous emission in the active plasmonic waveguide, one must first introduce the photocurrent operator. We assume that the photodetector of the receiver has an unlimited optical bandwidth and 100% quantum efficiency. In this case, the photocurrent is simply equal to the photon count rate multiplied by the electron charge. For example, for a single guided mode occupied by N quanta, the photocurrent J is equal to $Nv_g e/L$. Since the probability of photon detection is proportional to $\langle \hat{E}^-(t)\hat{E}^+(t)\rangle$, where $\hat{E}^-(t)$ and $\hat{E}^+(t)$ are the negative and positive frequency parts of the electric field operator [31], it is reasonable to define the photocurrent operator as

$$\hat{J} = \hat{\mathcal{E}}^-(t)\hat{\mathcal{E}}^+(t), \tag{8}$$

where

$$\begin{pmatrix} \hat{\mathcal{E}}^+(t) \\ \hat{\mathcal{E}}^-(t) \end{pmatrix} = \sum_i \sqrt{\frac{v_g(\beta_i)e}{L}} \begin{pmatrix} \hat{a}_i \exp(-2\pi i \nu_i t) \\ \hat{a}_i^\dagger \exp(2\pi i \nu_i t) \end{pmatrix}. \tag{9}$$

In the above expressions, $\hat{a}_i^\dagger$ and $\hat{a}_i$ are the creation and annihilation operators of the SPP states in the single-mode plasmonic waveguide. In Eq. (9), the summation is performed over the guided modes with only positive wave numbers ($\beta_i > 0$), since we are interested in the optical signal at the photodetector and neglect reflection from the waveguide facets.

The spectral density of noise produced by spontaneous emission can be derived from the autocorrelation function

$$\begin{aligned} B(\tau) &\equiv \langle \hat{J}(t)\hat{J}(t+\tau)\rangle \\ &= \langle \hat{\mathcal{E}}^-(t)\hat{\mathcal{E}}^-(t+\tau)\hat{\mathcal{E}}^+(t+\tau)\hat{\mathcal{E}}^+(t)\rangle. \end{aligned} \tag{10}$$

Using Eq. (9), the right-hand side of Eq. (10) can be represented as the sum of terms proportional to $\langle \hat{a}_{i_1}^\dagger \hat{a}_{i_2}^\dagger \hat{a}_{i_3}\hat{a}_{i_4}\rangle = N_{i_1}N_{i_2}(\delta_{i_1 i_3}\delta_{i_2 i_4} + \delta_{i_1 i_4}\delta_{i_2 i_3})$, where $\langle \hat{a}_i^\dagger \hat{a}_i\rangle \equiv N_i$:

$$\begin{aligned} B(\tau) = e^2 \sum_{i_1,i_2} \frac{v_g(\beta_{i_1})v_g(\beta_{i_2})}{L^2} N_{i_1}N_{i_2} \\ \times \{1 + \exp[-2\pi i(\nu_{i_1} - \nu_{i_2})\tau]\}. \end{aligned} \tag{11}$$

In this expression, there are terms that can be ascribed to the signal-spontaneous beat noise ($i_1 = 0$ or $i_2 = 0$):

$$B_{\text{s-sp}}(\tau) = e^2 \frac{N_0 v_g(\beta_0)}{L} \sum_i \frac{N_i v_g(\beta_i)}{L} 2\cos[2\pi(\nu_i - \nu_0)\tau] \tag{12}$$

and to the spontaneous-spontaneous beat noise ($i_1,\ i_2 \neq 0$),

$$\begin{aligned} B_{\text{sp-sp}}(\tau) = e^2 \sum_{i_1,i_2 \neq 0} \frac{v_g(\beta_{i_1})v_g(\beta_{i_2})}{L^2} \\ \times N_{i_1}N_{i_2} \exp[-2\pi i(\nu_{i_1} - \nu_{i_2})\tau]. \end{aligned} \tag{13}$$

The number N_i of SPP quanta with frequency ν_i at the photodetector can be found from the power P_0 of the SPP signal excited at the free-space wavelength λ_0 and the spontaneous emission spectrum at the receiver [see Eq. (5)]: $N_0 = P_0 L/[h\nu_0 v_g(\beta_0)]$ and $N_i|_{i\neq 0} = p_{\text{sp}}(h\nu_i)/\nu_i$.

We next replace the sums in expressions (12) and (13) by integrals using the rule

$$\sum_i \to \frac{L}{2\pi}\int d\beta \to \frac{L}{v_g}\int d\nu \tag{14}$$

and obtain the final expressions for the autocorrelation functions:

$$B_{\text{s-sp}}(\tau) = e^2 \frac{2P_0}{h\nu_0} \int_0^\infty \frac{p_{\text{sp}}(h\nu)}{h\nu} \cos[2\pi(\nu - \nu_0)\tau] d(h\nu), \tag{15}$$

$$B_{\text{sp-sp}}(\tau) = e^2 \int_0^\infty \int_0^\infty \frac{p_{\text{sp}}(h\nu_1)p_{\text{sp}}(h\nu_2)}{h\nu_1 h\nu_2} \times \exp[-2\pi i(\nu_1-\nu_2)\tau]d(h\nu_1)d(h\nu_2). \quad (16)$$

From these expressions, we can derive the power spectral density of noise using the Wiener-Khinchin theorem,

$$S_{\text{s-sp}}(f) = e^2 \frac{2P_0}{h\nu_0}\left[\frac{p_{\text{sp}}(h(\nu_0+f))}{\nu_0+f} + \frac{p_{\text{sp}}(h(\nu_0-f))}{\nu_0-f}\right], \quad (17)$$

$$S_{\text{sp-sp}}(f) = 2e^2 \int_0^\infty \frac{p_{\text{sp}}(h\nu)p_{\text{sp}}(h(\nu+f))}{\nu(\nu+f)}d\nu, \quad (18)$$

where f is the noise frequency. The maximum noise frequency f is limited by the RC rise time of the receiver circuit and is much smaller than the optical frequency ν_0; therefore, expressions (17) and (18) can be simplified to

$$S_{\text{s-sp}}(f) \approx e^2 \frac{4P_0 p_{\text{sp}}(h\nu_0)}{h\nu_0^2}, \quad (19)$$

$$S_{\text{sp-sp}}(f) \approx 2e^2 \int_0^\infty \frac{p_{\text{sp}}(h\nu)^2}{\nu^2}d\nu. \quad (20)$$

Here we note that the simplified expression (19) has been previously derived for optical amplifiers by Olsson [30] using the classical approach under the additional assumption of a uniform amplifier gain over a narrow optical bandwidth. Using this assumption, expression (20) can also be reduced to that derived by Olsson.

Finally, one needs to take into account the shot noise originating from the discrete nature of electrons [32]. Its power spectral density is given by $S_{\text{shot}}(f) = 2eJ$. Despite that the shot noise is not directly determined by the spontaneous emission, it depends on the net photocurrent J, which is a function $J = J(P_0, P_{\text{sp}})$ of the signal power P_0 and the spontaneous emission power P_{sp}.

Equations (17), (18), and (5) clearly show that the noise power increases as the length of the waveguide with gain increases. In the deep-subwavelength waveguide in the regime of full loss compensation, the material gain in the semiconductor is high and so is the spontaneous emission rate at the photodetector. For this reason, the signal-spontaneous beat noise is noticeable even at a small waveguide length of 10 μm [see Fig. 4(a)] exceeding the shot noise for $P_0 = 100$ μW, which is a characteristic value for state-of-the-art on-chip communication systems [33–36]. $S_{\text{s-sp}}$ shows a linear dependence on the signal power P_0 and the waveguide length L. As P_0 decreases, the power of the signal-spontaneous beat noise also decreases, but this does not affect the spontaneous-spontaneous beat noise [Fig. 4(b)], which depends only on the spontaneous emission power [see Eq. (20) for details]. In contrast to long-range active plasmonic waveguides [7], where the SPP modal gain G does not exceed 30 cm^{-1}, in deep-subwavelength active plasmonic waveguides, the role of the spontaneous-spontaneous beat noise is crucial due to the relatively large bandwidth of the spontaneous emission spectrum in the semiconductor active medium [Fig. 3(a)] and the high SPP modal gain [$G(h\nu_0) = \alpha(h\nu_0) = 1300$ cm^{-1}]. $S_{\text{sp-sp}}$ is proportional to the 3/2 power of the waveguide length and dominates over $S_{\text{sp-sp}}$ for $L > 10.5$ mm at $P_0 = 100$ μW. As the signal power decreases tenfold, which is highly beneficial for the energy efficiency of active plasmonic devices, the influence of $S_{\text{sp-sp}}$ becomes stronger and $S_{\text{s-sp}} = S_{\text{s-sp}}$ at $L = 130$ μm.

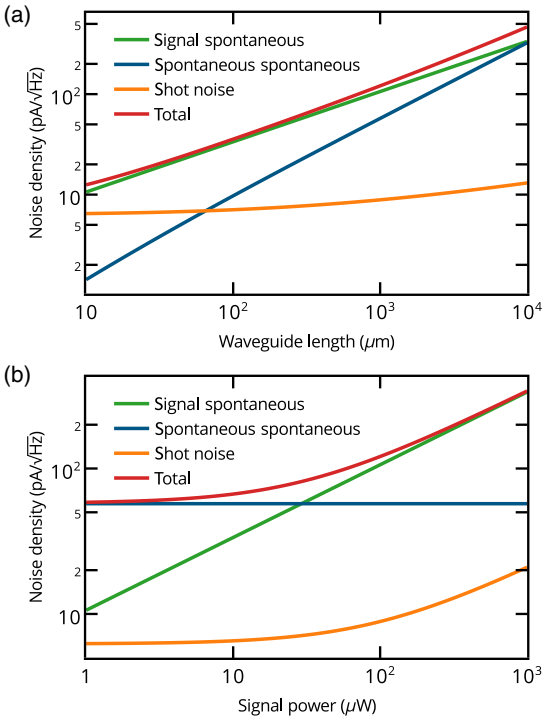

FIG. 4. (a) Power spectral density of noise at the photodetector as a function of the length of the active plasmonic waveguide shown in Fig. 2(a). The signal power is equal to 100 μW, $\lambda_0 = 1550$ nm. (b) Power spectral density of noise at the photodetector versus signal power at a fixed waveguide length of 1 mm.

To evaluate the influence of the spontaneous emission noise on the performance of deep-subwavelength active plasmonic waveguides, we directly calculate the root-mean-square (rms) current fluctuation using the Parseval equation:

$$\text{rms}_J = \sqrt{\int_0^\infty [S_{\text{s-sp}}(f) + S_{\text{sp-sp}}(f) + S_{\text{shot}}(f)]|\chi(f)|^2 df}, \quad (21)$$

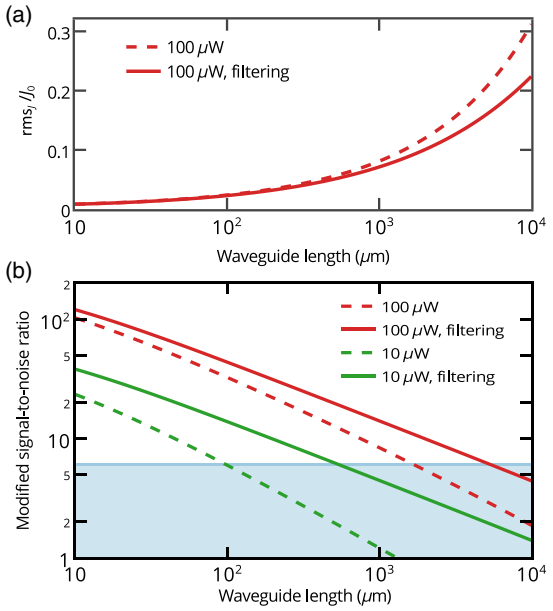

FIG. 5. (a) Normalized rms current noise at the photodetector as a function of the waveguide length, $P_0 = 100$ μW. (b) Dependence of signal-to-noise ratio on the waveguide length for two different signal powers. In both panels, the solid curves correspond to the system with a narrow bandpass optical filter, and the dashed curves correspond to the systems without optical filters.

where $\chi(f)$ is the response function of the receiver. For simplicity, we assume that $\chi(f)$ is equal to 1 within the spectral bandwidth W_e of the receiver ($f < W_e$) and is zero elsewhere. Figure 5(a) shows the obtained normalized fluctuation of the photocurrent as a function of the length of the deep-subwavelength active plasmonic waveguide shown in Fig. 2(a). We also plotted the rms current fluctuation for the photodetector combined with a bandpass optical filter, which is an essential element for optical communication technologies [34]. Filtering gives the possibility to cut off most of the spontaneous emission spectrum and suppresses the spontaneous-spontaneous beat noise. At the same time, the power of the signal-spontaneous beat noise is not affected by optical filtering, since only SPP quanta with a frequency within a very narrow (approximately $2W_e$) band around ν_0 can contribute to the signal-spontaneous noise as follows from Eq. (17).

The performance of the communication line is determined by the bit error ratio (BER), which is a measure of the percentage of bits that are not transmitted or received correctly. The BER is a function of the modified signal-to-noise ratio (MSNR) [29] given by

$$\mathrm{MSNR} = \frac{J|_{P=P_0} - J|_{P=0}}{\mathrm{rms}_J|_{P=P_0} + \mathrm{rms}_J|_{P=0}}. \tag{22}$$

When $\mathrm{rms}_J|_{P=0} \ll \mathrm{rms}_J|_{P=P_0}$, which can be realized using a bandpass optical filter, expression (22) simplifies to

$$\mathrm{MSNR} \approx \frac{J|_{P=P_0}}{\mathrm{rms}_J|_{P=P_0}} = \mathrm{SNR}, \tag{23}$$

where SNR is the well-established classical signal-to-noise ratio.

The required BER depends on the communication protocol. Modern protocols typically deal with communication lines, where the BER is lower than 10^{-9}, which corresponds to MSNR > 6. If the MSNR drops to less than 6, it is still possible to establish a very high-speed and reliable connection [37], but technical realization is usually very complicated. Assuming the SPP signal power is equal to 100 μW, which technically corresponds to an energy of 10 fJ in the optical pulse (approximately 8000 SPP quanta or photons, which is a characteristic value for the state-of-the-art on-chip communication systems [33–36]) at a bit rate of 10 Gbit/s (one pulse per bit), assuming the electrical bandwidth of the photodetector to be as high as 7 GHz, which is sufficient for reliable detection [38], we can obtain the modified signal-to-noise ratio for the active plasmonic waveguide shown in Fig. 2(a). Figure 5(b) demonstrates that the spontaneous emission noise does not present a problem for on-chip communication in this case. Assuming that the energy of the optical pulse can be reduced tenfold in the future, we find that communication over distances longer than 1 mm can be complicated, and special optimization techniques may be needed. One can also switch to a different waveguide geometry, such as a hybrid plasmonic waveguide, which provides about 30% longer communication distance for similar dimensions of the waveguides. Another possible solution to extend the communication distance is to increase the operation wavelength λ_0 and proportionally increase the waveguide dimensions [see Fig. 2(a)]. As λ_0 increases, the Ohmic losses in the metal decrease, and, consequently, the properly adjusted ternary (InGa)As alloy gives fewer SPP quanta into the waveguide mode. Figure 6 shows

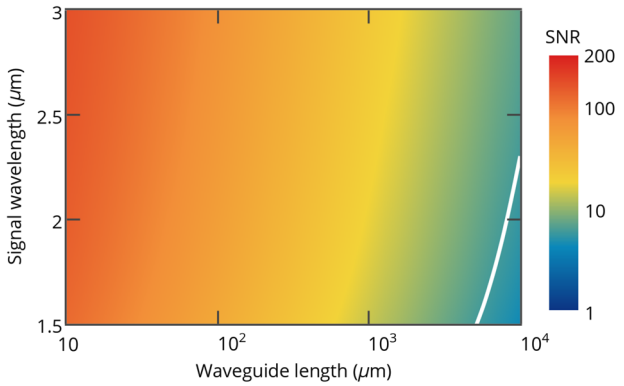

FIG. 6. Signal-to-noise ratio at the receiver as a function of the operation wavelength λ_0 and the length of the active plasmonic waveguides. The white curve corresponds to SNR $= 6$, which separates the regions with BER $< 10^{-9}$ (to the left of the curve) and BER $> 10^{-9}$ (to the right of the curve).

the signal-to-noise ratio versus the signal wavelength and the waveguide length assuming the same number (approximately 8000) of SPP quanta per bit in the optical signal. It is clearly seen that by increasing the operation wavelength λ_0 from 1550 nm to 3 μm, it is possible to increase the communication distance threefold. In addition, operation at longer wavelengths gives better energy efficiency, but the mode size of the SPP mode is certainly slightly larger than at shorter wavelengths.

In the above analysis, we consider only inherent properties of the plasmonic waveguide with gain. However, in practical communication lines, one should take into account the nonzero coupling loss α_{coupl} between the waveguide and the photodetector and the nonunity quantum efficiency η_{phd} of the photodetector. In this case, the power densities of noise given by Eqs. (17) and (18) should be multiplied by $[(1-\alpha_{\mathrm{coupl}})\eta_{\mathrm{phd}}]^2$, while the shot noise and the signal current are changed by a factor of $(1-\alpha_{\mathrm{coupl}})\eta_{\mathrm{phd}}$ [32]. As a result, the shot noise is promoted relative to the beat noise. However, at practical waveguide lengths, the shot noise is much weaker than the beat noise (see Fig. 4), and the signal-to-noise ratio and BER remain almost unaffected.

IV. SUMMARY

We present a theoretical framework within which the spontaneous emission power and the spontaneous emission noise can be evaluated in plasmonic waveguides with gain and in SPP amplifiers. The developed framework can be easily applied with no change to active plasmonic or nanophotonic waveguides of any shape and level of mode confinement. The equations are valid for a wide range of active media, which includes semiconductors, quantum wells, low-dimensional semiconductors, dye molecules, rare-earth ions, etc. Using the developed theory and numerical simulations, we obtain the characteristics of deep-subwavelength metal-semiconductor plasmonic waveguides, which can simultaneously provide deep-subwavelength (approximately $\lambda^2/130$) mode confinement and full compensation of the SPP propagation loss. The net SPP gain in such a waveguide is equal to zero for the signal and is negative for the spontaneous emission. For this reason, in contrast to optical amplifiers, the spontaneous emission is not amplified; however, the material gain in the active medium required for loss compensation is very high, which results in a very broad and intense spontaneous emission. The total spontaneous emission at the end of the waveguide is the same order of magnitude as the signal power, which significantly affects the noise characteristics of the deep-subwavelength plasmonic waveguide with gain. In addition, the spectrum of spontaneous emission at the end of the waveguide is very broad, which is significantly different from the typical situation in optical amplifiers [7,20,30,32]. For this reason, using the quantum-optics formalism, we derive accurate expressions to address the noise produced by the spontaneous emission with a broad and nonuniform spectrum. The spontaneous-spontaneous beat noise is very strong, dominating over the signal-spontaneous beat noise and seriously limiting the maximum communication distance, which is critical for practical applications. At the same time, we demonstrate that the spontaneous-spontaneous beat noise can be suppressed using optical filtering techniques, while the signal-spontaneous beat noise, which cannot be filtered, can be controlled at a level sufficient for a wide range of on-chip applications.

ACKNOWLEDGMENTS

This work is supported by the Russian Science Foundation (Grant No. 14-19-01788).

[1] S. Bozhevolnyi, *Plasmonic Nanoguides and Circuits* (Pan Stanford Publishing, Singapore, 2009).
[2] K. Leosson, Optical amplification of surface plasmon polaritons: Review, J. Nanophoton. **6**, 061801 (2012).
[3] P. Berini and I. De Leon, Surface plasmon–polariton amplifiers and lasers, Nat. Photonics **6**, 16 (2011).
[4] D. Y. Fedyanin and A. V. Arsenin, Semiconductor surface plasmon amplifier based on a Schottky barrier diode, AIP Conf. Proc. **1291**, 112 (2010).
[5] D. Costantini, A. Bousseksou, M. Fevrier, B. Dagens, and R. Colombelli, Loss and gain measurements of tensile strained quantum well diode lasers for plasmonic devices at telecom wavelengths, IEEE J. Quantum Electron. **48**, 73 (2012).
[6] T. Suhara, *Semiconductor Laser Fundamentals* (CRC Press, New York, 2004).
[7] I. De Leon and P. Berini, Theory of noise in high-gain surface plasmon-polariton amplifiers incorporating dipolar gain media, Opt. Express **19**, 20506 (2011).
[8] I. De Leon and P. Berini, Spontaneous emission in long-range surface plasmon-polariton amplifiers, Phys. Rev. B **83**, 081414(R) (2011).
[9] L. Thylen, P. Holmstrom, A. Bratkovsky, J. Li, and S.-Y. Wang, Limits on integration as determined by power dissipation and signal-to-noise ratio in loss-compensated photonic integrated circuits based on metal/quantum-dot materials, IEEE J. Quantum Electron. **46**, 518 (2010).
[10] F. Vallini, Q. Gu, M. Kats, Y. Fainman, and N. C. Frateschi, Carrier saturation in multiple quantum well metallo-dielectric semiconductor nanolaser: Is bulk material a better choice for gain media?, Opt. Express **21**, 25985 (2013).
[11] W. W. Chow and S. W. Koch, *Semiconductor-Laser Fundamentals: Physics of the Gain Materials* (Springer Science & Business Media, New York, 2013).
[12] H. C. Casey and M. B. Panish, *Heterostructure Lasers: Part A* (Academic Press, New York, 1978).
[13] T. D. Visser, H. Blok, B. Demeulenaere, and D. Lenstra, Confinement factors and gain in optical amplifiers, IEEE J. Quantum Electron. **33**, 1763 (1997).

[14] A. A. Vyshnevyy and D. Y. Fedyanin, Self-heating and cooling of active plasmonic waveguides, ACS Photonics **3**, 51 (2016).
[15] D. Y. Fedyanin, A. V. Krasavin, A. V. Arsenin, and A. V. Zayats, Surface plasmon polariton amplification upon electrical injection in highly integrated plasmonic circuits, Nano Lett. **12**, 2459 (2012).
[16] A. V. Krasavin and A. V. Zayats, Active nanophotonic circuitry based on dielectric-loaded plasmonic waveguides, Adv. Opt. Mater. **3**, 1662 (2015).
[17] R. F. Oulton, V. J. Sorger, D. A. Genov, D. F. P. Pile, and X. Zhang, A hybrid plasmonic waveguide for subwavelength confinement and long-range propagation, Nat. Photonics **2**, 496 (2008).
[18] A. Andryieuski, V. A. Zenin, R. Malureanu, V. S. Volkov, S. I. Bozhevolnyi, and A. V. Lavrinenko, Direct characterization of plasmonic slot waveguides and nanocouplers, Nano Lett. **14**, 3925 (2014).
[19] D. A. Svintsov, A. V. Arsenin, and D. Y. Fedyanin, Full loss compensation in hybrid plasmonic waveguides under electrical pumping, Opt. Express **23**, 19358 (2015).
[20] P. M. Becker, A. A. Olsson, and J. R. Simpson, *Erbium-Doped Fiber Amplifiers: Fundamentals and Technology* (Academic Press, New York, 1999).
[21] K. Tanaka, T. Kazuo, T. Masahiro, and S. Tatsuhiko, Simulation of practical nanometric optical circuits based on surface plasmon polariton gap waveguides, Opt. Express **13**, 256 (2005).
[22] H. Temkin, T. Tanbun-Ek, and R. A. Logan, Strained InGaAs/InP quantum well lasers, Appl. Phys. Lett. **56**, 1210 (1990).
[23] J. Treu, T. Julian, S. Thomas, W. Marc, M. Stefanie, D. Markus, M. Sonja, S. Kai, B. Max, A. Gerhard, J. J. Finley, S. Julian, and K. Gregor, Lattice-matched InGaAs–InAlAs core–shell nanowires with improved luminescence and photoresponse properties, Nano Lett. **15**, 3533 (2015).
[24] R. L. Williams, M. Dion, F. Chatenoud, and K. Dzurko, Extremely low threshold current strained InGaAs/AlGaAs lasers by molecular beam epitaxy, Appl. Phys. Lett. **58**, 1816 (1991).
[25] D. Y. Fedyanin, D. I. Yakubovsky, R. V. Kirtaev, and V. S. Volkov, Ultralow-loss CMOS copper plasmonic waveguides, Nano Lett. **16**, 362 (2016).
[26] K. M. McPeak, S. V. Jayanti, S. J. P. Kress, S. Meyer, S. Iotti, A. Rossinelli, and D. J. Norris, Plasmonic films can easily be better: Rules and recipes, ACS Photonics **2**, 326 (2015).
[27] R. Ho, K. Mai, and M. Horowitz, Efficient On-Chip Global Interconnects, in *Proceedings of 2003 Symposium on VLSI Circuits* (IEEE, New York, 2003).
[28] D. N. Klyshko and A. V. Masalov, Photon noise: Observation, squeezing, interpretation, Phys. Usp. **38**, 1203 (1995).
[29] L. N. Binh, *Photonic Signal Processing: Techniques and Applications* (CRC Press, New York, 2007).
[30] N. A. Olsson, Lightwave systems with optical amplifiers, J. Lightwave Technol. **7**, 1071 (1989).
[31] M. O. Scully and M. Suhail Zubairy, *Quantum Optics* (Cambridge University Press, Cambridge, England, 1997).
[32] N. K. Dutta and Q. Wang, *Semiconductor Optical Amplifiers* (World Scientific, Singapore, 2013).
[33] S. Manipatruni, M. Lipson, and I. A. Young, Device scaling considerations for nanophotonic CMOS global interconnects, IEEE J. Sel. Top. Quantum Electron. **19**, 8200109 (2013).
[34] C. Sun *et al.*, Single-chip microprocessor that communicates directly using light, Nature (London) **528**, 534 (2015).
[35] A. Narasimha *et al.*, A 40-Gb/s QSFP Optoelectronic Transceiver in a 0.13 μm CMOS Silicon-on-Insulator Technology, in *Proceedings of the Conference on Optical Fiber Communication/National Fiber Optic Engineers* (IEEE, New York, 2008).
[36] D. A. B. Miller, Optical interconnects to electronic chips, Appl. Opt. **49**, F59 (2010).
[37] R. W. Hamming, Error detecting and error correcting codes, Bell Syst. Tech. J. **29**, 147 (1950).
[38] J. P. Dakin and R. G. W. Brown, *Handbook of Optoelectronics* (CRC Press, New York, 2010).